ARTICLE

TECHNOLOGY

Asymmetric voltage multiplying circuit coupled to sliding electrodes for biomass fractionation with high-voltage and high current pulsed electric fields

Klimentiy Levkov & Alexander Golberg

Pulsed electric field (PEF) is an emerging technology for biomass processing and fractionation by electroporation of cell membrane. Nevertheless, PEF technology and devices require tailoring and adaptation for each specific type of biomass. Such an optimization requires convenient and adaptable laboratory systems, which will enable both electrical and mechanical parameters determination before process upscaling. In this work, we report on the design and development of a laboratory PEF system that allows applying for up to 4 kV, 1 kA pulses with 1–100 μs and total power dissipation of 20 W and up to 25 kg of mechanical load. The design of an asymmetric voltage multiplying circuit allows for controlling pulse parameters for each pulse in series. Such an approach enables precise adaptation of PEF to the changing conductivity of the biomass, minimizing the total invested energy in the process. The system was tested on highly conductive marine macroalgae *Ulva* sp, a promising but challenging feedstock for the biorefinery. This work provides a design of an adaptable PEF device, important for biomass processing with electroporation.

***Keywords*: Pulsed Electric Field Generator; Electroporation; Biomass Processing; Macroalgae; Bioeconomy.**

INNOVATION

High-voltage pulsed electric fields (PEFs) increase the permeability of the cell membrane thus enabling the separation of liquid and solid phases of the biomass. This process saves energy by direct water extraction and also extracts valuable intracellular compounds. However, unique physical characteristics of each species of plant biomass, the dynamics and nature of their changes in the process of electroporation require a case-by-case adaptation of PEF parameters such as applied voltage, number of pulses, pulse duration, frequency and temperature for successful and energy efficiency biomass fractionation. Unfortunately, there are few devices available today at the laboratory scale, which provide sufficient flexibility to determine these basic benchmarks that are necessary for the upscaling of PEF systems for industrial-scale biomass processing. The goal of this work is to design and develop a laboratory-scale device, which allows gaining the data necessary for developing technologies and technical systems for large-scale biomass processing. The developed PEF device allows determining the changes in the biomass volume measuring continuously the interelectrode gap and impedance of the electroporated biomass measuring the current changes as a function of the specific applied mechanical pressure, pulse voltage amplitude, pulse duration, the number of pulses, and pulse repetition rate. The novel asymmetric voltage multiplying circuit allows to control voltages at each pulse as a function of biomass condition; thus, minimizing the applied energy. The system was tested on the electroporation of highly conductive green seaweed *Ulva* sp. biomass. Such a device will enable the rapid optimization of the PEF process parameters required for upscaling.

ABBREVIATIONS

EPC		electroporation cell
HVPG		the high-voltage pulse generator
GPED		the gravitational press-electrode device
V	[cm^3]	volume of EPC
Z	[Ohm]	biomass impedance in the EPC
U_E	[Volt]	amplitude value of electroporation pulse voltage
t_P	[sec]	duration of electroporation pulse voltage
F	[Hz]	electroporation voltage pulse repetition rate
P	[kg cm^{-2}]	specific electrode pressure on electroporated biomass
N		the number of current pulses acting on the biomass
$V_{O(max)}$	[Volt]	maximum operating voltage of the switch

Porter School of Environment and Earth Sciences, Tel Aviv University, Tel Aviv, Israel. Correspondence should be addressed to: A.G. (agolberg@tauex.tau.ac.il).

Received 12 December 2019; accepted 3 August 2020; published online 27 August 2020; doi:10.1142/S2339547820500016

$I_{P(max)}$	[A]	maximum peak current of the switch
R_{CL}	[Ohm]	the resistance of a current-limiting resistor
V_{SAT}	[Volt]	typical saturation voltage of the switch
I_L	[Amp]	maximum continuous current of the switch
$P_{D(max)}$	[Watt]	maximum continuous power dissipation of switch
LTD	[Watt/°C]	linear temperature derating of $P_{D(max)}$
T_o	[°C]	temperature range
R_{DC}	[Ohm]	the resistance of the discharge circuit of the ESC
U_{em}	[Volt]	the maximum value of electroporation voltage
I_{em}	[Amp]	maximum value of electroporation current
I_P	[Amp]	effective value (rms value) of pulse current in the discharge circuit
P_{pd}	[Watt]	pulse power dissipated at the switch
t_{pm}	[sec]	maximum pulse duration
U	[Volt]	value of the voltage accumulated on the ESC
U_0	[Volt]	the voltage on the ESC before the current pulse is applied
U_{ESC}	[Volt]	the voltage on the ENC after the current pulse is applied
C_{ESC}	[farad]	the capacitance of the energy storage capacitor
W	[Watt]	the required power of the high-voltage source
U_{TR}	[Volt]	the output voltage of the step-up transformer
I_{TR}	[Amp]	the output current of the step-up transformer
U_{VD}	[Volt]	the output voltage of the voltage doubler
Z_{CC}	[Ohm]	the impedance of the charging circuit
X_C	[Farad]	capacitive resistance of the charging capacitor
C_{CL}	[Farad]	the capacitance of the charging and current-limiting capacitor
K_F		the form factor of the sinusoidal current
U_{TM}	[Volt]	output voltage of a high-voltage transformer
W_{DC}	[Watt]	the energy that is dissipated in the discharge circuit during the current pulse action
R_{SW}	[Ohm]	the resistance value of the high-voltage switch (HV SWITCH)
R_{BM}	[Ohm]	the current biomass resistance value
U_{BM}	[Volt]	effective value (rms value) of pulse voltage on the biomass
W_{BM}	[Watt]	the amount of energy dissipated in the electroporated biomass during the current pulse action
W_{SW}	[Watt]	the amount of energy dissipated in the high-voltage switch during the current pulse action

INTRODUCTION

Growing population in improving lifestyles requires industrial growth, challenging food, chemicals, and energy sectors. Growth in these major economic sectors increases negative environmental impacts. One of the possible solutions to these challenges is the sustainable production and conversion of biomass[1]. Bioeconomy is the emerging sector of the economy, which aims to develop sustainable biomass-based products for energy, food, and chemical sectors[2,3]. However, multiple technological challenges are needed to be solved to implement the vision of sustainable bioeconomy[1,4,5].

Of the major technological challenges for bioeconomy is biomass fractionation, or biorefining: similar to oil or gas cracking or refining[6]. An important step in biomass fractionation is the breakdown of cell membranes[7,8]. This breakdown allows for efficient separation of liquid from organic material (drying) and also it enables to extract for various useful intercellular components such as proteins, amino acids, lipids, carotenoids, and other molecules with significant market values[9,10]. One type of technology for cell membrane rupture is based on the high-voltage, short PEF[11].

Used first in the 1930s[12,13] for sugar extraction from sugar beets, PEF technology and processes recently gained momentum leading to several industrial-scale implementations[14,15] such as potato,[16–18] tomato,[19] sugar beets[20–22], and grape[23,24] processing[11]. Although the exact mechanism of biological tissue permeabilization by PEF is not fully understood, PEF technology is also currently used in multiple applications in medicine and biotechnology[25,26]. The current theory suggests that the membrane permeabilization is achieved through the formation of aqueous pores on the cell membrane, a phenomenon known as electroporation[27].

However, unique physical characteristics of each species of plant biomass, the dynamics and nature of their changes in the process of electroporation require a case-by-case adaptation of PEF parameters such as applied voltage, number of pulses, pulse duration, frequency, and temperature for successful and energy efficiency biomass fractionation. Unfortunately, very few devices are available today[28–30] at the laboratory scale, which provides sufficient flexibility to determine these basic benchmarks that are necessary for developing technologies and technical systems for biomass processing[30,31].

Detailed reviews summarized the current state of the art of equipment development for electroporation and PEFs applications[30,32–35]. Puc *et al.* conducted broad research on the available on the market electroporation devices and described in detail their functionality, advantages, and disadvantages[36]. In brief, generators of the high-voltage PEF can be classified into three major groups: transformers, capacitors, and resonant inverters[32]. Although transformer-based devices can achieve high voltages[37], they cannot generate arbitrary waveforms and are limited to specific amplitude and frequency that are preset[32]. Also, the waveform they generate is not precise and thus can lead to unpredicted biomass electroporation results and consume extra energy for the process. Capacitor-based inverters use a capacitor bank to store energy plus a switch to deliver a unipolar/bipolar output voltage[38]. Topologies including single-stage voltage source inverters (VSIs), and modular multilevel systems, required for high-voltage output, have been proposed[39–42]. Also, different special topologies, including Marx generators and Blumlein networks[43] have been proposed for nanosecond pulse duration generators[44,45]. In **Table 1,** we summarized the properties and operational parameters of some of the recently published high-voltage pulse generator (HVPG) topologies. Even though multiple topologies have been proposed in the literature, none of them allows adaptation of applied voltage during the delivery of pulse series on biomass-based biomass conditions. Besides, none of them allows for optimization of required PEF parameters requires for biomass processing scale-up. In addition, most of the reported devices allow for limited current applications, thus preventing their use on the marine macroalgae, which have very low conductivity and thus require the operation of both high-voltage and high-current protocols.

The goal of this work is to design and develop a laboratory-scale device, which will allow gaining the data that are necessary for developing technologies and technical systems for large-scale biomass processing. The developed prototype is designed to determine the changes in the volume (V) and impedance (Z) of the electroporated biomass, depending on the specific electrode pressure (P), pulse voltage amplitude (U_E), pulse duration (t_P), the number of pulses (N), and pulse repetition rate (F). The device was tested on marine macroalgae biomass, an emerging feedstock for biorefinery[52–56]. Indeed, macroalgae fractionation with

Table 1 Properties and operational parameters of some of the recently published high-voltage pulse generator topologies. A detailed review of the commercial instrumentation appears in Ref[36].

Type	Max voltage	Max current	Pulse duration	Frequency	Efficiency	Ref.
Transformer	10 kV	NA	5 µs	1 kHz	67%	Tseng *et al.*[37]
	1 kV	NA	500 ns			
Modular multilevel capacitor	4 kV	150 A	10–100 µs			Sarnago *et al.*[46]
	1.275 kV	20 A	10 µs–10 ms	1 Hz–50 kHz		Petkovsek *et al.*[42]
MOSFET	3 kV	50 A	Up to 1 ms			Bertacchini *et al.*[47]
	3 kV	60 A	100 ns–1 ms	1 Hz to 3.5 MHz		Novickij *et al.*[48]
	5 kV	80 A	10 µs–10 ms	1–10 Hz		Flisar *et al.*[49]
H-bridge topology	1 kV	100 A	1 µs–10 ms			Grainys *et al.*[50]
Frozen wave generator concept using photoconductive semiconductor switches	1 kV 6.9 kV 4 kV		2 ns 9.2 ns 745 ps		20%–100%	Kohler *et al.*[44]
Blumlein configuration	0.25–1 kV		20–300 ns	1.1 MHz		Reberek *et al.*[43]
30-stage Marx generator with IGBT switches	1 kV	500 A				Sack *et al.*[29]
Sinusoidal generator	2400 Vpp		5 ms	1 MHz		Garcia-Sanchez *et al.*[51]

PEFs, once available, could lead to nonthermal, chemical-free extraction and concentration of valuable phytochemicals from cells such as proteins, amino acids, and carbohydrates[57–60]. However, macroalgae biomass is the most challenging feedstock for PEF application in the industry because of high salinity (38 g L^{-1}), which leads to the very low resistance of the biomass and very high currents in the system at fields that lead to cell membrane permeabilization[58,61].

RESULTS AND DISCUSSION

A high-level description of the developed laboratory-scale PEF system with sliding electrodes

The schematic representation of the key elements of the developed system is shown in **Fig. 1.** The system consists of four major elements:

1) **Charging device:** Zero voltage switch power controller and zero voltage power switch for connecting the grid control and high-voltage transformer (HV-TR) that supplies charge for capacitors; voltage doubler to enable step charging of the energy storage capacitor, enabling voltage control of each pulse. This voltage control is needed to address the dynamics of the resistance of the electroporated biomass.
2) **Energy storage capacitor (ESC):** Capacitor, discharging resistor, for safety and charge control for each pulse, and high-voltage switch used for pulse shape control.
3) **Electroporation cell (EPC):** Chamber with electrodes applied to the biomass.
4) **Microcontroller:** A control unit that regulates the shape and energy for each pulse based on the biomass conductivity and volume.

The details of these modules will be discussed in the following sections.

The technical requirements for the laboratory installation: 4000 V, 1.5 kA, 1–100 µs pulse duration, determined the construction of its mechanical, electrical, and software parts. These parameters were chosen based on our previous studies of seaweed electroporation[57] to allow electroporation optimization for various biomass cakes thicknesses (up to 1 cm).

The developed laboratory system consists of several circuits and mechanical nodes that must provide the process of registering data for constructing the following functional dependencies that will be used in large-scale devices:

- Changing the volume of biomass and its impedance as a function of pressure (without electroporation):

$$V = f(P),\ Z = f(P),\ (U_E,\ t_p,\ N,\ F) = 0; \quad (1)$$

where U_E is the applied voltage (Volts), t_p (µs) is the duration of the pulse, N is the number of pulses, P is the applied mechanical pressure (kg m^{-2}), Z is the biomass impedance (Ohm), V is the biomass volume between the electrodes (cm^3).

- Changing the volume of biomass and its impedance as a function of pressure for fixed values of the impulse voltage, the duration of pulses, and their number

$$V = f(P),\ Z = f(P),\ (U_E,\ t_p,\ N,\ F) = \text{Constant}. \quad (2)$$

- Changing the volume of biomass and its impedance as a function of applied voltage at constant pressure, the duration of pulses, and their number

$$V = f(U_E),\ Z = f(U_E),\ (P,\ t_p,\ N,\ F) = \text{Constant}. \quad (3)$$

- Change in the volume of biomass and its impedance as a function of the length of pulses at constant pressure, the magnitude of the impulse voltage, and the number of pulses

$$V = f(t_p),\ Z = f(t_p),\ (P,\ U_E,\ N,\ F) = \text{Constant}. \quad (4)$$

- Change in the volume of biomass and its impedance as a function of the number of pulses at constant pressure, the magnitude of the impulse voltage, and the duration of pulses

$$V = f(N),\ Z = f(N),\ (P,\ U_E,\ t_p,\ F) = \text{Constant}. \quad (5)$$

- Changing the volume of biomass and its impedance as a function of the repetition rate of pulses

$$V = f(F),\ Z = f(F),\ (P,\ U_E,\ t_p,\ N) = \text{Constant}. \quad (6)$$

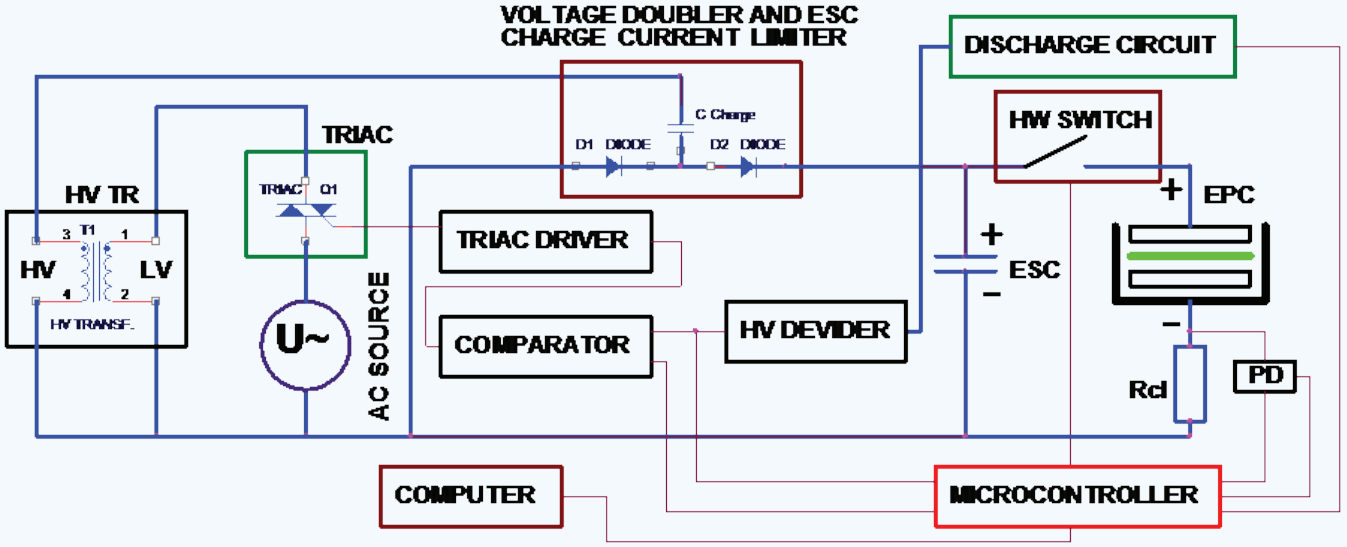

Figure 1 Conceptual scheme of the laboratory pulsed electric field-based device for biomass electroporation.

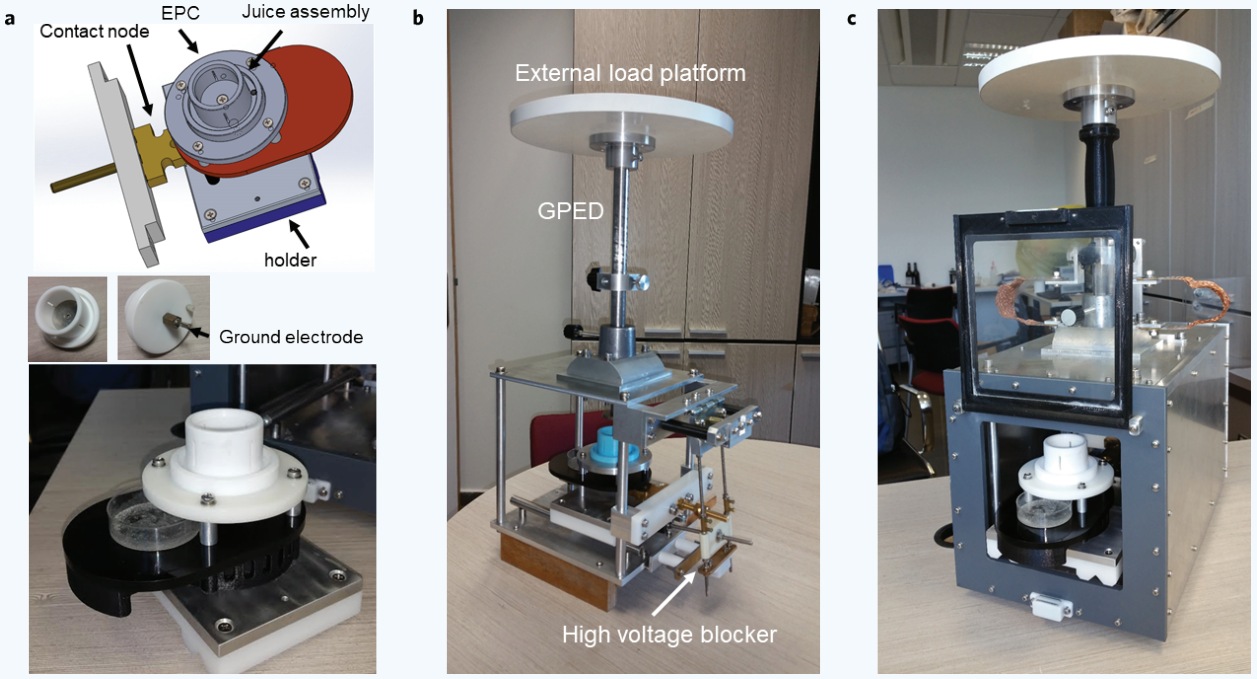

Figure 2 Electroporation cell. (**a**) The top figure shows the design of the EPC module. Bottom digital images show the final EPC with contact electrodes. (**b**) The gravitational press-electrode device. (**c**) High-voltage chamber assembly.

High-voltage chamber

The main nodes of the mechanical part of the developed laboratory device are EPC (**Fig. 2a**), EPC holder (**Fig. 2a),** the contact assembly of the EPC, the gravity press-electrode device (with the sliding electrode), and a high-voltage blocker (**Fig. 2b**). All these units are mounted in the housing of the high-voltage chamber (**Fig. 2c**). EPC is designed to hold the biomass in the interelectrode space during the process of electroporation, as well as the separation of biomass into liquid and solid cake simultaneously with the application of electric fields.

The EPC (**Fig. 2a**) node consists of three parts: a plastic body (Teflon) of a cylindrical shape (2.5 cm diameter), the positive electrode (stainless steel), located at the lower part of the cylinder, and the plug-type contact

for the connection with power supply. In the lateral part of the EPC body, there are four narrow slit-shaped openings 1.5 mm wide for the exit of the liquid fraction during the electroporation squeezing of biomass (**Fig. 2a**). The extracted juice is collected and poured through a groove at the base of the EPC. Using plug-in contact, the EPC is connected to the fixation node inside the high-voltage chamber.

The EPC holder (**Fig. 2a**) is needed for its electrical connection to the output of a HVPG, mechanical fixation, and positioning inside a high-voltage chamber. The positioning or precise installation of the EPC inside the high-voltage chamber is necessary to combine the axis of the positive fixed electrode with the axis of the negative mobile electrode. In addition, the EPC fixing unit can be easily installed and removed from the high-voltage chamber by sliding (**Fig. 2c**) without the use of tools. This is very convenient for replacing of the biomass in the laboratory environment. The functions of the contact node are to provide a plug-in high-voltage and high-current contact of the EPC holder with a HVPG, as well as providing positioning of the EPC. It consists of a specially designed contact pair, insulating board, and fixation parts (**Fig. 2a**).

The gravitational press-electrode device with a sliding electrode (GPED, 1604 g) is shown in **Fig. 2b**. With the help of the GPED, an interelectrode pressure is maintained before, during, and after the application of PEF. For this, GPED is made in the form of a vertically disposed rod that slides easily in a stationary cage. The load-receiving platform is fixed at the upper end of the rod and a movable negative electrode, which can freely move inside the EPC is connected to its lower end. A load weighing up to 25 kg can be placed on the load-receiving platform to create the necessary interelectrode pressure on the biomass (**Fig. 2b**). A displacement sensor (optoNCDT, Micro-Epsilon, NC), **Fig. 2c** is installed on the GPED to monitor the volume change of the biomass during electroporation.

The high-voltage blocking device (**Fig. 2b**) is necessary to ensure the safe operation of the system in a laboratory environment. It is installed in the rear of the high-voltage chamber (**Fig. 2b**) and works by a locking mechanism. The mechanism of high-voltage blocking device is equipped with a microswitch for the electrical circuit of high-voltage switching, a HVPG output blocking contact, and contact of the discharge circuit of ESCs.

The assembled high-voltage chamber is shown in **Fig. 2c.** It is designed for precise positioning of EPC under the negative movable electrode, its fixation, and also for creating conditions for safe operation. Once EPC is inserted inside the chamber, it is impossible to reach the high-voltage parts by hand. All the above mechanical components are integrated into the high-voltage chamber, as well as cables and connectors for connection to a HVPG. Because of the guides and the special contact unit, accurate positioning of the EPC fixing unit under the minus electrode is done by a single click. During the experiments, the high-voltage chamber is closed with a transparent door (**Fig. 2c**).

The high-voltage high-current pulse generator

The main functional nodes of the electrical system are:

- Two parallel-connected ESCs with a total capacity of 100 μF for a voltage of 6 kV (Maxwell, CA, cat#34083, custom made).
- High-voltage source of charge of ESCs.
- Circuit node of the discharge of ESCs.
- High-voltage contactor for the pulsed discharge of ESC on electroporated biomass.
- Circuit node for manual control of high-voltage contactor in testing mode.
- Circuit nodes for providing voltage measurements on the ESC, on the EPC and the electroporation current.
- Microcontroller.

The electrical part of the device is connected, through the microcontroller, by an interface with the computer for implementing programmable experiments on electroporation of biomass. The displacement sensor, which is mounted on a GPED, is connected to the control computer by a separate interface.

The HVPG is designed to carry out the electroporation of biomass by acting on it with current pulses of high voltage. The immediate formation of high-voltage and high-current pulses is carried out by a high-voltage switch (**Fig. 3**). For this, rectangular pulses are fed to its control input. In the test mode, single pulses are sent from the circuit node with the manual control, and in the programmable experiment mode from the microcontroller.

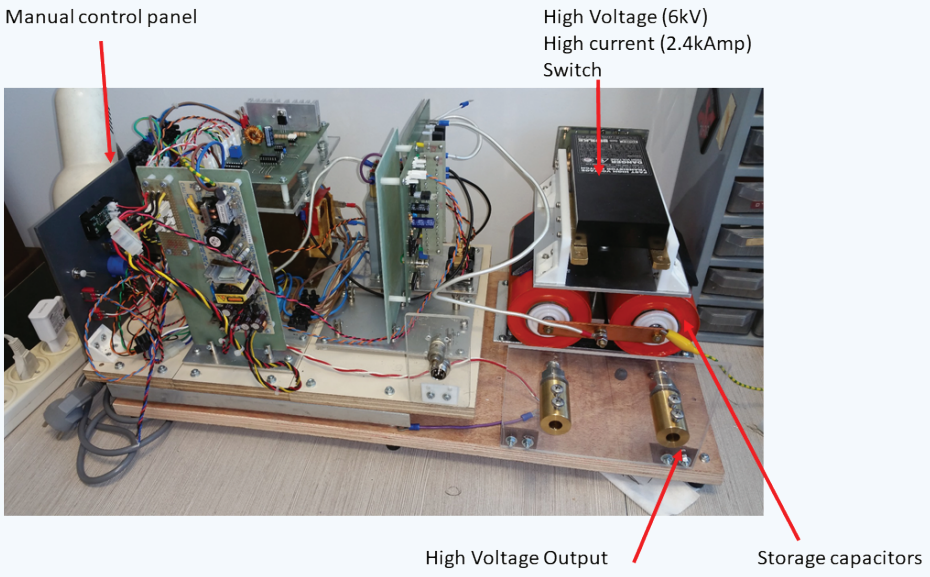

Figure 3 High voltage pulse generator. Digital image.

The most important functional elements of the electrical circuit are a high-voltage switch, ESC, as well as a high-voltage charge source of an ESC. The following section describes the principles for their selection in this work.

High-voltage switch

The choice of a high-voltage contractor is determined by the maximum voltage and impulse current. Preliminary analysis of the maximum rated voltage of high-voltage elements in impulse devices should be at least 33% higher than the working voltage. This is related to the impulse resonance excess of the voltage (spikes), which occurs in the operating mode. Thus, at a required operating voltage of 4 kV, the maximum voltage of the switching element must be 6 kV.

The choice of the maximum pulse current is determined by the value of the biomass impedance. According to the measurements, the impedance of

the electroporated macroalgae biomass can be in the range from 1.5 to 20 Ohm for an electrode with areas from 2.5 to 10 cm^2, with biomass layer from 1 to 20 mm, and various electrolytic conductivity of the biomass. The values of these resistances, which are also dynamic, because of biomass electroporation, determine a wide range of current load, which, in the absence of current limitation, can reach over 4 kA in a pulse. In addition, with a possible electrical breakdown of the biomass, a short-circuit current occurs, which can reach destructive values. In this case, it is necessary to select a switching element with the largest possible admissible pulse current. In addition, active or passive current limiting is necessary, which protects the used switching element from failure.

Based on the analysis described in the previous section, and comparison of characteristics, for the laboratory device we selected fast high-voltage transistor switch HTS 61-240-SI for voltage 6 kV and current 2.4 kA (BEHLKE, Germany). However, in this switch, as in all such devices, there is no possibility of active current limitation. Therefore, a series connection of a low-inductance resistor, calculated for the maximum impulse current, is necessary to provide for passive current limiting in the discharge. For a current of 2.4 kA, with a possible pulse exceeding the voltage up to 6 kV, a resistor whose resistance is equal to 2.5 Ohm was chosen ($R = U_m / I_m = 6000/2400 = 2.5$ Ohm; FPA250, 2.5 Ohm, 250 Watt, ARCOL, UK).

An additional important factor that determines the nature of the operation of a high-voltage switching element is its thermal regime. In the general manual for the use of BEHLKE high-voltage contactors for thermal conditions, the following is written: "Thermal Overload. Switching frequency, pulse cycle, load capacitance, and working resistance are to be chosen in such a way that thermal overload is avoided. HTS switches are fitted with a sensor to protect them from over-temperature conditions which will inhibit operation of the switch when an internal temperature of 70°C is detected. Since the temperature sensor is relatively sluggish on account of the thermal isolation, a fast uncontrolled increase in temperature can cause damage to the switch. Especially in the case of laboratory set-ups, there is the danger that too high frequencies are set accidentally at the signal generator or too high voltages at the laboratory high-voltage power supply. For this reason, the current at the HV supply must be limited." These recommendations determined the need for an analysis of the thermal parameters of the fast high-voltage transistor switch HTS 61-240-SI.

The power that this switch must dissipate is determined by the mode of operation of the plant for electroporation of the biomass: the current amplitude, the frequency, and the duration of the pulses. The thermal model of the high-voltage contactor is determined using six parameters, which are given in the technical description on the HTS 61-240-SI. The first parameter is maximum peak current (I_{Pmax}), which can be $I_{P(max)}$ = 2400 A with pulse duration t_p <= 100 µs. The second parameter is the typical saturation voltage (V_{sat}). At the pulse current $0.1 \cdot I_{Pmax}$; V_{sat} = 18 V. At a pulse current of $1.0 \cdot I_{P(max)}$; V_{sat} = 120 V. The third parameter defines the maximum continuous current (I_L). For the switch used, HTS 61-240-SI, it is equal to I_L = 3.0 A. The fourth parameter is maximum continuous power dissipation ($P_{D(max)}$), the dissipation power of a high-voltage switch, which is open for a long time with a nonpulsed current of 3 A and equal to 25 W for HTS 61-240-SI at 25°C. The fifth parameter—linear temperature derating of $P_{D(max)}$. LTD = 0.55 W/°C—determines the decrease in the energy parameters of the impact on the function of the contactor temperature. The sixth parameter is temperature range (T_o) = −30 ... + 70°C.

The saturation voltage (voltage drop across the switch) is equal to $V_{sat} = P_{D(max)} / I_L = 25/3 = 8.333$ V. The saturation voltage depends on the pulse current, and the released heat, which depends on the pulse duration. At a current of $0.1 \cdot I_{P(max)}$, equal to 240 A, the saturation voltage increases and is equal to 18 V. The power dissipation, at the switch, when a single pulse of 100 µs duration is fed at a current of 240 A, will be $P_D = V_{sat} \cdot I_P \cdot t_p = 18 \cdot 240 \cdot 0.0001 = 0.432$ W. Within a permissible 25 W, this allows feeding $N = 25 / 0.432 = 57.87$ such pulses per second. Thus, the maximum frequency for this case is $F = 57.87$ Hz.

At a maximum pulse current of $1.0 \cdot I_{Pmax}$ equal to 2400 A, the saturation voltage is equal to V_{sat} = 120 V. When one pulse of 100 µs duration is fed, the power dissipation at the switch will be $P_D = V_{sat} \cdot I_P \cdot t_p = 120 \cdot 2400 \cdot 0.0001 = 28.8$ W. This switch heating power determines the maximum pulse repetition rate $F = 25/28.8 = 0.868$ Hz. Naturally, shorter pulses make it possible to increase the frequency of the current pulses with the invariance of its amplitude.

The heating of the switch determines the need to reduce the energy parameters of electroporation following LTD of $P_{D(max)} = 0.55$ W/°C. For example, with increasing the switch heating by 10°C, the power dissipation must be reduced by 5.5 W. Accordingly, if the power dissipation at the switch is higher than a new $P_{D(max)}$ will be equal to 25 − 5.5 = 19.5 W. Therefore, the current (I_p) of the pulses, or their duration (t_p) or the frequency (F) should be reduced.

It is desirable to determine the permissible repetition rate of pulses or the values of the pulses duration and their currents as a function of the heating of the high-voltage contactor. This dependence should be built into the control program for monitoring the set parameters and for correcting the parameters of electroporation in real time. This function was not implemented at this point in the laboratory device.

One of the parameters that are not sufficiently defined in the technical description for this purpose is the dependence of the saturation voltage of the switch (V_{sat}) on the value of the impulse current (I_p).

In principle, two points are given at switch documentation: at the pulse current $0.1 \cdot I_{P(max)}$ (240 A); V_{sat} = 18 V, and at a pulse current of $1.0 \cdot I_{P(max)}$ (2400 A); V_{sat} = 120 V. Assuming linear behavior of the switch in this system the to approximate the I-V characteristic is given by:

$$V_{sat} = 0.04722 \cdot I_P + 6.667. \quad (7)$$

For example, at a maximum current pulse (I_{em}) of electroporation 500 A and V_{sat} = 30.277 V; then, with a pulse duration of 100 µs, the power it allocates will be $P_{pd} = V_{sat} \cdot I_P \cdot t_p = 30.277 \cdot 500 \cdot 0.0001 = 1.514$ W. In this case, the maximum pulse rate (F) can be set for this electroporation mode $F = P_{D(max)}/P_{pd} = 25/1.514 = 16.512$ Hz.

In the selected fast high-voltage transistor switch HTS 61-240-SI, there is protection against overheating, which stops its operation when reaching an unacceptable temperature. However, the real mode of operation of this device requires constant temperature control to correct the values of individual parameters of electroporation. For this purpose, a temperature sensor output is required that is absent in this type of contactor. In the absence of direct temperature control, it is necessary to use the computational method, which is realized based on the current–voltage characteristic of V_{sat} as described above. For this purpose, a corresponding subprogram is located in the software of the controlling microcontroller, using which certain parameters of the electroporation are corrected and regulated in real time.

ENERGY STORAGE CAPACITOR

The choice of the type of ESC is determined by the maximum voltage, the maximum value of the impulse current load, the minimum value of the intrinsic inductance, and the repetition rate of the pulses. In addition, the value of the capacity of the ESC is determined by the allowable decrease in the voltage on the ESC after the maximum current pulse and the maximum duration of the current pulse.

We set the maximum values of the voltage and current of the ESC, as well as the maximum pulse duration, respectively, U_{em} = 4 kV, I_{em} = 1 kA, and t_p = 100 µs. For these maximum parameters, we accept the allowable voltage drop on the ESC after a current pulse of 1 kA for 100 µs duration equal to 25%. Following the specified parameters, the minimum value of the resistance of the discharge circuit of the ESC is $R_{DC} = U_{em}/I_{em} = 4 \cdot 10^3/1 \cdot 10^3 = 4$ Ohm. From this value, 2.5 Ohm is the resistance

of a current-limiting resistor as described above. The voltage drop after a current pulse of 25% of 4 kV corresponds to 3000 V. In this case, the value of the ESC capacity (C_{ESC}) should be

$$C_{ESC} = t_p / (\ln U_0 - \ln U_{ESC}) \cdot R_{DC} = 100 \cdot 10^{-6} / (\ln 4000 - \ln 3000) \cdot 4 = 100 \cdot 10^{-6} / (8.294 - 8.006) \cdot 4 = 86.806 \text{ uF} \quad (8)$$

where t_p is the duration of the pulse, U_0 is the voltage on the ESC before the current pulse is applied, U_{ESC} is the voltage on the ESC after the current pulse is applied. Based on the calculation, we accept the nearest larger standard value of the capacity of the ESC equal to $C_{ESC} = 100$ µF.

ESC CHARGING SOURCE

The choice of the parameters of the ESC charge source is determined by the maximum value of the voltage, current, and pulse duration in process electroporation of the biomass. The pulse repetition frequency is set taking into account the permissible heating and the conditions for cooling the biomass in the EPC as described above. Given the maximum voltage parameters $U_{em} = 4000$ V, the current $I_{em} = 1000$ A, and the pulse width $t_p = 100$ µs, we take the pulse frequency $F = 1$ Hz. Therefore, the required power of the source must be at least

$$W = U_{em} \cdot I_{em} \cdot t_p \cdot F = 4 \cdot 10^3 \cdot 1 \cdot 10^3 \cdot 100 \cdot 10^{-6} \cdot 1 = 400 \text{ W} \quad (9)$$

At a voltage of 4000 V, a pulse current of 100 A and a pulse duration of 10 µs with the same ESC power source power, the pulses repetition rate can be increased to 100 Hz.

It should be borne in mind that the presence of a 2.5 Ohm passive current-limiting resistor lowers the process energy efficiency (η) as

$$\eta = Z/(Z + R_{CL}) \quad (10)$$

where the Z—biomass impedance in the EPC, which is predominantly resistive; R_{CL}—resistance of a current-limiting resistor.

In addition to the basic parameters of the ESC charge source, which are voltage and power, when choosing it, it is necessary to take into account the availability of such necessary functions as:

- Regulation of the voltage of the ESC charge.
- Prohibition and resolution of ESC charging.
- Control of output voltage.
- An indication of charging completion.
- Overheating indication, and so on.

The developed device uses a charge source, which consists of a step-up transformer of 220/2000 V, a voltage doubler, and an ESC voltage regulating unit. With the help of a voltage doubler, the output voltage (U_{TR}) of the transformer can be increased to the maximum value of U_{VD} as follows

$$U_{VD} = \sqrt{2} \cdot 2U_{TR} = \sqrt{2} \cdot 2 \cdot 2000 = 5657 \text{ V}. \quad (11)$$

The developed device uses an asymmetric voltage doubling circuit, which consists of two high-voltage diodes and two capacitors. This is a new feature, we did not found in the literature. The first is a charging capacitor that, in addition to the voltage doubling function, performs the function of current limitation when the ESC is charged. The second capacitor is ESC. The choice of the capacity of the charging capacitor is determined by the requirements that are related to:

- The fulfillment of the current limitation function for ESC charging.
- Ensuring the necessary power of the electroporation process.
- Ensuring the acceptable accuracy of the electroporation voltage setting.

With the required power of 400 W and a voltage of 2000 V, the output current of the transformer must be at least: $I_{TR} = W/U_{TR} = 400/2000 = 0.2$ A. The total resistance of the charging circuit in this case is $Z_{cc} = U_{TR}/I_{TR} = 2000/0.2 = 10 \cdot 10^3$ Ohm. If we neglect the relatively small internal resistance of the transformer, then the resistance of the charging circuit is determined by the capacitive resistance of the charging capacitor X_C, which is assumed equal to Z_{cc}.

Taking into account the half-wave rectification of the alternating current in the voltage doubler, as well as the conversion when rectifying the effective value of the sinusoidal alternating current into its average value, the capacitance of the input capacitor (C_{CL}) is determined:

$$C_{CL} = 2 \cdot K_F/2\pi \cdot F \cdot X_C = 2 \cdot 1.11 / 6.28 \cdot 50 \cdot 10 \cdot 10^3 = 0.71 \text{ uF} \quad (12)$$

where $K_F = 1.11$ is the form factor of the sinusoidal current. The closest standard value of the charging capacitance $C_{CL} = 0.7$ uF is selected.

The charging capacitor is connected to the output of a HV-TR with a maximum secondary voltage $U_{TM} = \sqrt{2} \cdot U_{TR} = 1.414 \cdot 2000 = 2828$ V. The required standard value of the working voltage of the charging capacitor must be at least this value. The high-voltage capacitor CH85-21070 for microwave ovens with voltage AC RMS 2100 V (3000 V DC) was chosen as a charging capacitor.

The process of ESC charge using a voltage doubler occurs according to the exponential law (**Fig. 4a**).

$$U_{ESC} = 1 - U_{VD} \cdot \exp(-t/X_C \cdot C_{ESC}) \quad (13)$$

An increase in the voltage on the ESC occurs at each half-cycle of the sinusoidal voltage when the charging capacitor is recharged. The process of ESC charge has a discrete and portioning character, which is depicted in **Fig. 4b**, enable voltage control for each pulse. A discrete voltage increment occurs on the ESC every half-cycle. The magnitude of this increment depends on the difference between the accumulated and maximum voltage.

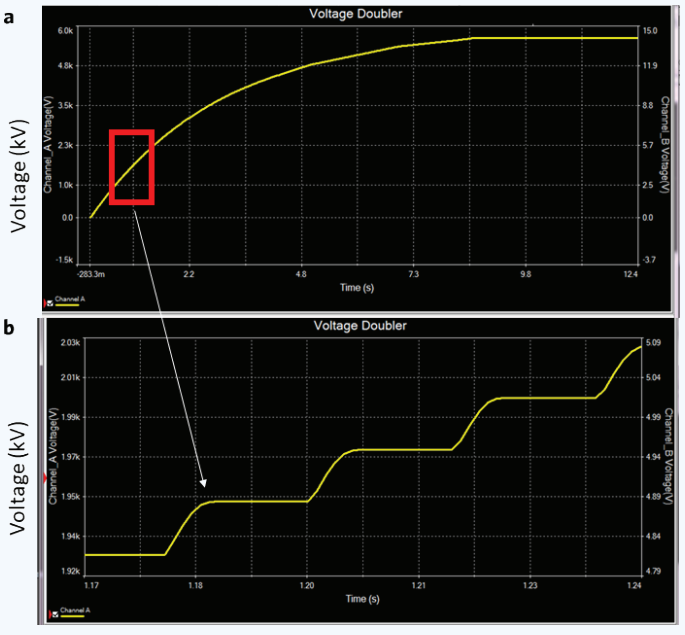

Figure 4 ESC charge using a voltage doubler. (**a**) Low resolution. (**b**) High resolution shows the principle of step (quantum) charging using asymmetrical design.

The value of the discrete voltage increments (dU) in the process of ESC charge is described by the inversely proportional function

$$dU = \frac{C_{CL} U_{VD}}{C_{ESC}} \cdot \left(1 - \frac{U_{ESC}}{U_{VD}}\right) \quad (14)$$

In the developed system, C_{CL} is the capacitance of the current-limiting charge capacitor (0.7 μF); C_{ESC}—the capacity of the ESC (100 μF); U_m—the value of the maximum doubled voltage (5657 V); U—the value of the voltage accumulated on the ESC (600–4000 V).

For example, a discrete increment of voltage on the ESC for one period at an existing voltage $U = 1000$ V will be $dU = 34.8$ V. With the accumulated voltage $U = 2000$ V, the voltage on the ESC will be equal to $dU = 29.7$ V. At $U = 3000$ V, $dU = 23.25$ V, and at $U = 4000$ V, $dU = 15.7$ V. In another example, a discrete increment of voltage on the ESC for one period at an existing voltage $U_{ESC} = 0$ V will be $dU = 39.6$ V. With the accumulated voltage $U_{ESC} = 1000$ V, the voltage on the ESC will be equal to $dU = 32.6$ V. At $U_{ESC} = 2000$ V, $dU = 25.6$ V. At a voltage $U_{ESC} = 3000$ V, $dU = 18.6$ V, and at $U_{ESC} = 4000$ V, $dU = 11.6$ V. Thus, within a range of voltages required for electroporation, the charge source can theoretically provide the accuracy of the voltage setting from 5% to 0.4%, depending on the voltage value on the ESC.

The voltage required for the electroporation on the ESC is set by the method of discrete control of charge using an electrical circuit of comparing the set and actual voltage.

CIRCUIT CONTROL OF THE DEVELOPED LABORATORY PULSE GENERATOR

The electrical circuit of the unit ensures its operation in the mode of test and computer control. The test mode is set by the switch on the control panel. In the test mode, the voltage is set using the potentiometer located on the front panel, and then a single or repeated press of the test single pulse button. The test pulses are fed to the electrical equivalent of the EPC, or the biomass loaded to the EPC. Adjustable in the test mode high voltage is monitored using a panel voltmeter. Wherein, with the help of a special switch, both the installed and the actual voltage on the ESC are monitored in real time. In addition, the electrical circuit of the installation allows observation and recording of the voltage and current pulses using external devices.

Figure 1 shows its functional diagram in computer control mode. The HV-TR, the bidirectional triode thyristor (TRIAC), and the voltage doubler that charge the ESC to the specified voltage. The ESC is both an element of the voltage doubler and a working measure of capacitance for indirect measurement of current and dissipated energy in the elements of the discharge circuit. The voltage doubler, in addition to performing the function of increasing voltage, performs the function of limiting the charge current ESC. Using the HV SWITCH, the ESC is connected to the electrodes of the EPC for a predetermined time. The device also implements the principle of passive current limitation. For this, a powerful low-inductance current-limiting resistor $R_{CL} = 2.5$ Ohm is implemented in the discharge circuit. The purpose of this resistor is to limit the current in the discharge circuit in the event of a short circuit. This resistor is also a current-measuring shunt. The voltage pulse from the current-limiting resistor is fed to the input of the peak detector PD.

The purpose of the peak detector is to fix the maximum current value in the discharge circuit, which in the case of a short circuit allows you to quickly stop the pulse supply process without a command from the computer. The ESC charging processes and the delivery of electroporation pulses are controlled by a microcontroller. The bidirectional triode thyristor (TRIAC) is controlled by its driver.

The triac driver is the zero voltage switch controller. It carries out the inclusion of a triac during the transition of an alternating voltage through zero. This prevents inrush currents and overvoltages at the transformer output when the triac is turned on. The comparator compares the voltage specified from the analog output of the microcontroller with the voltage that comes from the output of the ESC voltage divider. If the voltage on the ESC is lower than the set value, then the output of the comparator is set to a high level and triac opens by means his driver. In this case, the ESC charge occurs until the specified voltage is reached. When the voltage on the ESC reaches a predetermined value, then the output of the comparator is set low and the triac is locked by mean his driver.

This leads to the termination of the charging process ESC.

Electric discharge of ESC to electroporate biomass is performed for a specified time period.

In shape, this discharge represents a rectangular pulse of current and voltage with exponential decay.

The voltage at the ESC is measured using the ADC of microcontroller before applying the electroporation pulse to the biomass and after it is completed. These direct measurements are transferred to a computer for calculations, the result of which is a complex of indirect measurements of the discharge circuit current, electroporation voltage on the biomass, as well as the level of energy loss in the biomass and in the high-voltage switch. If the energy loss in the biomass or in the high-voltage switch exceeds the permissible values, then in the necessary proportion, the pulse repetition rate is automatically reduced. In this case, the corresponding message is displayed on the computer screen. To ensure safe operation with the device, it uses a software-controlled functional node "DISCHARGE CIRCUIT," which is connected to the microcontroller, which performs a full discharge of ESC at the end of the working cycle. Therefore, the functions of the microcontroller include direct control of the cyclic process of electroporation, providing direct measurements and an interface with a computer.

Computer functions include:

- The initial input of electroporation parameters and their correction upon entry.
- Transfer of the entered parameters to the microcontroller.
- Transmission of the commands "START EXPERIMENT" and "STOP EXPERIMENT."
- Transmitting to the microcontroller a command for correcting the pulse repetition rate during the experiment to implement the function of protecting against overheating of biomass or a high-voltage switch.
- Receiving from the microcontroller the current parameters of the experiment, their processing, and recording to the registration file for subsequent analysis.
- Display on the screen of the current parameters of the experiment in digital and graphic form.

The receipt and processing of information, that comes from the microcontroller to the computer, is performed by him during a pause between pulses. During this period the following parameters are calculated:

a) The current value of the resistance of the discharge circuit:

$$R_{DC} = t_p / (\ln U_0 - \ln U_{ESC}) \cdot C_{ESC} \quad (15)$$

b) The amount of energy that is dissipated in the discharge circuit during the current pulse action:

$$W_{DC} = 0.5 \cdot C_{ESC} \cdot (U_0^2 - U_{ESC}^2) \quad (16)$$

c) Root mean square (rms) value of pulse current in the discharge circuit

$$I_P = V(W_{DC} / R_{DC} \cdot t_p) \quad (17)$$

d) Resistance value of the high-voltage switch (HV SWITCH)

$$R_{SW} = 0.04722 + 6.67 / I_P \quad (18)$$

e) The current biomass resistance value

$$R_{BM} = R_{DC} - R_{CL} - R_{SW} \quad (19)$$

f) The magnitude of the maximum electroporation voltage, which is applied to the biomass

$$R_{BM} = R_{DC} - R_{CL} - R_{SW} \quad (20)$$

g) Rms value of pulse voltage on the biomass

$$U_{BM} = I_P \cdot R_{BM} \quad (21)$$

h) The amount of energy dissipated in the electroporated biomass during the current pulse action

$$W_{BM} = W_{DC} \cdot R_{BM} / R_{DC} \quad (22)$$

i) The amount of energy dissipated in the high-voltage switch during the current pulse action

$$W_{SW} = W_{DC} \cdot R_{SW} / R_{DC} \quad (23)$$

Images of the voltage and current pulses as recorded applying 2 kV (field ~2 kV/cm), 12 µs duration 200 A (±10 A) on 10 g of wet macroalgae are shown in **Fig. 5a. Figure 5b** shows the algae biomass loaded in the high-voltage chamber. This is in the range of electric field requirement shown in our previous work to extract proteins from this biomass[57]. Besides a challenging marine macroalgae biomass, those parameters of PEF could be used to electroporation multiple types of biomass such as sugar beets and agricultural wastes[11].

The procedure for biomass electroporation is carried as followings:

1. Loading the biomass inward the EPC outside the device.
2. Installing the EPC together with the biomass in the EPS fixing unit.
3. Installing the EPC together with its fixing unit in a high-voltage chamber. With the correct installation of this unit in a high-voltage chamber, a microswitch of high-voltage blocker closes its contact, which allows turn on a high-voltage source.
4. With help from the GPED, the negative electrode the lowered into the EPC until full mechanical contact with the loaded biomass.
5. The external load with a certain mass for a particular experiment is installing onto a load-receiving platform to create mechanical pressure on the biomass.
6. The "TEST/WORK" switch switches to the "TEST" position for periodic testing of the device in manual mode.
7. Testing of the device in manual mode.

   The standard testing load of 10 or 100 Ohm is connected to the HVPG output.
   By pressing the button "HV ON," the high-voltage source is switched on.
   By periodically pressing the "TP" button, a series of pulses fed to the load.
   Using an amperometric probe and an oscilloscope, the correspondence of the magnitude of the pulse current to the value of the voltage set on the ESC is determined.
   After testing, by pressing the "HV OFF" button, the high voltage is turned off and the ESC is discharged.
   The test load is disconnected and a high-voltage chamber is connected to the HVPG output (**Fig. 2**).
8. The switch "TEST/WORK" is switching to the position "WORK" to continue the process in the mode of control by microcontroller and computer.
9. Determining the status of the device. It must be turned on and connected to the computer. If this condition is not met, a corresponding message appears on the computer screen.
10. Checking the position of the "TEST/WORK" switch and indicating its position on the computer screen. If the switch "TEST/WORK" is in the position "TEST," then to continue the process in computer control mode, it must be transferred to the position "WORK."
11. Entering the initial parameters of the experiment:
    - voltage of electroporation pulses (600–4000 V);
    - duration of electroporation pulses (from 5 to 100 µs);
    - the maximum pulse repetition rate of 100 Hz with an allowable dissipated power on the biomass and the high-voltage switch;
    - the number of pulses of electroporation;
    - area of electrodes (2.5, 5, 10 cm^2);
    - the external mechanical load (from 2 to 25 kg);
    - the weight of biomass loaded in the EPC before the experiment;
    - the date and time of the beginning and completion of the experiment are entered automatically when creating the registration file of experiment results;
    - short name (designation) of the experiment;
    - name and location on the disk of the file to record the results of the experiment.

    In the process of setting of input parameters, the computer program checks their permissible values, mutual correspondence, and also matches the heating and cooling conditions of the switching device and biomass in the EPC.
    The settings data is assigned to the corresponding constants and variables.
    The format of created files for recording the results of the experiment contains the header part and data columns.
    The identification and the initial parameters entered are recorded in the header part of this file.
12. After completing the input of the initial parameters of the experiment, a click is made on the "START EXPERIMENT" button of the graphical interface of the computer program.

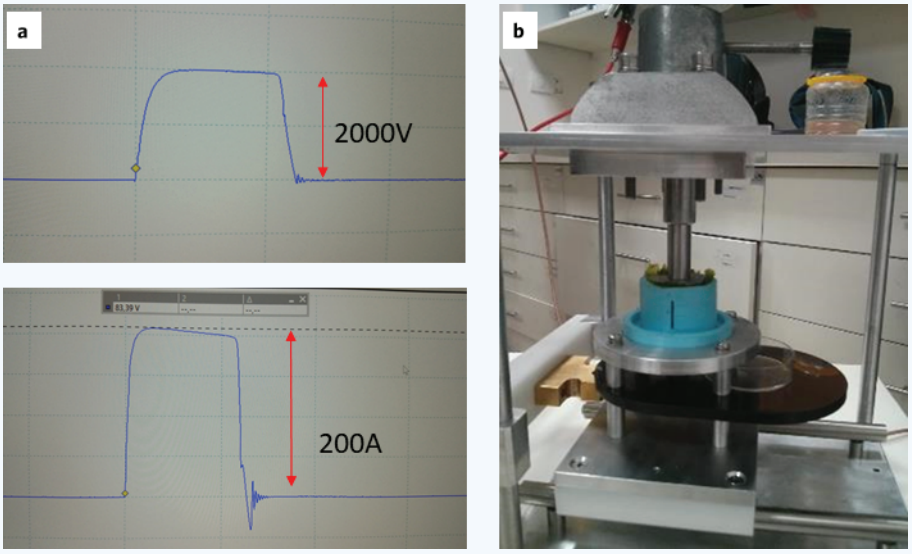

Figure 5 (**a**) Voltage (top image) and current (bottom image) of *Ulva* biomass exposed to pulsed electric fields of 2 kV. (**b**) Loaded in electroporation cell *Ulva* biomass. Digital image.

13. After clicking on the "START EXPERIMENT" button, the initial parameters of the experiment are transferred to the HVPG microcontroller and a file for recording the results of the experiment is created. When creating this file, the contents of the header part are entered into it.
    The computer program sends a command to start the duty cycle to the microcontroller.
14. In the process of the work cycle, the microcontroller and computer program perform:
    a) in the microcontroller: zeroing of a digital-to-analog converter (0–5 V), which controls the value of the pulse voltage;
    zeroing of a timer, which sets the value of the pulse duration;
    zeroing of the timer, which sets the value of the time interval between pulses; resetting of the pulse counter;
    b) a smooth (within 2–3 seconds) increase in the control voltage until the set value of the electroporation voltage;
    c) when charging the ESC, when the voltage on it reaches the set value, the charging process stops, and the value U_0 is assigned to this value;
    d) at the command of the microcontroller opens HV SWITCH and high voltage from ESC connects to EPC;
    if a short circuit current was detected when connecting a high voltage to the EPC, the pulse supply process stops with the corresponding message being displayed on the computer screen;
    in case of a short circuit in the discharge circuit, after the supply of pulses ceases, the ESC charge ceases and its discharge is performed;
    in the normal state of the discharge circuit starts a timer, on which the value of the specified pulse duration has been set;
    when this timer completes the countdown of the set pulse duration, a close command is issued HV SWITCH;
    e) the second timer of the microcontroller starts, which sets the time interval between pulses;
    f) the analog–digital converter of the microcontroller measures the residual voltage on the ESC and its measured value is assigned to the variable U_{ESC};
    g) the signal of the prohibition of charging of the ESC is removed, which corresponds to the command for charging it to a predetermined value of voltage;
    h) the measured voltage values U_0 and U_{ESC} are transmitted to the computer;
    i) during a pause between pulses, the computer processes and writes to the file the information received from the microcontroller;
    the graphical interface panel of the computer program displays the values of the current parameters of the electroporation process in digital and graphical forms;
    j) the number of pulses N acting on the biomass is checked;
    if this quantity is equal to the set, then go to step o;
    if the number of pulses applied to the biomass is less than the specified one, then the content of the program counter of pulses is increased by one and a new value is assigned to the variable N;
    the state of the "STOP EXPERIMENT" flag is checked;
    if this flag is in the active state (the operator clicked on the "STOP EXPERIMENT" button), then go to step o;
    k) if, as a result of computer calculations, the excess of the allowable power dissipation is determined in the electroporated biomass or the high-voltage switch, then a proportional decrease in the pulse repetition rate is performed;
    in this case, the corresponding command is sent from the computer to the microcontroller;
    by the microcontroller, during a pause between pulses, the magnitude of the voltage achieved during the charge on the ESC is checked;
    l) if the specified voltage on the ESC was not reached during the established pause between pulses, then perform a jump to step. l;
    m) after the end of the pause between pulses and the achievement of a given voltage on the ESC, the transition to step c;
    n) exit from the working cycle after completion of the supply to the biomass of the specified number of pulses or at the initiative of the operator (cessation of feed impulses and charging ESC);
    o) output to the graphical interface of the computer program the message about the completion of the electroporation cycle;
    p) on command from the computer, a full discharge of ESC is performed.
15. After the experiment is completed, the high-voltage charge source of ESC is turned off by pressing the "HV OFF" button.

From the high-voltage chamber, the EPC fixation assembly is extracted.

This leads to the opening of the interlocking contact, which makes it impossible to turn on the high voltage without the EPC fixation unit installed in the high-voltage chamber.

An additional safety measure is to connect the active HVPG output to the ground when there is no EPC fixation unit in the high-voltage chamber.

SUMMARY

In this work, we developed the technical requirements for a laboratory installation for research in the field of electroporation of biomass and its functional structure that meets these requirements; design of the EPC and its holder; the concept of construction and design of a high-voltage camera; electrical schematic diagram of the laboratory device; principles of selection of high-voltage and high-current electrical circuit elements. However, the conducted tests of the designed unit on marine biomass showed its low energy efficiency on the electroporation marine biomass (which has a very low resistance of 5 Ohm). This limits the use of the device in experiments with the area of an electrode of more than 2.5 cm^2, as well as in experiments with marine biomass directly in the seawater (currently washing in the freshwater is needed). The reason for the low efficiency is the need for passive current limitation for the high-voltage contactor fast high-voltage transistor switch HTS 61-240-SI, which is used in the designed device. Passive current limiting is achieved by a series connection to the used contactor of a powerful low-inductance resistor of 2.5 Ohm. Also, the absence of effective cooling in this switch causes the productivity of the device insufficient for continuous electroporation of macroalgae in the seawater. In subsequent developments, it is necessary to find alternatives to the standard high-voltage modules that do not provide the necessary current limitation for their protection against overloads and short-circuit currents, as well as their effective cooling and current temperature control.

The developed ESC charging source based on the step-up transformer for microwave ovens showed its performance up to a maximum voltage of 5 kV. Its advantage is the simplicity of the technical solution and the low cost. The disadvantages of the applied source, its dimensions, and weight should be noted, the relatively low accuracy of voltage regulation of low levels (up to 1500 V), as well as the minimum adjustable voltage, which cannot be less than 600 V. It is also desirable to increase the charge rate to more than 50 Hz current acceptable from the grid. This is planned to be achieved by increasing the frequency of the charging current by adding a frequency converter. Also, an increase in the frequency of the charging current will significantly reduce the dimensions and weight of the source.

The applied voltage doubling circuit is modified to perform the additional function of the current limiting of the ESC when it is charged in combination with the requirements for the accuracy of voltage regulation. To do this, it did asymmetrically. Acceptable for current limitation and accuracy of voltage regulation, ESC asymmetry is achieved with the ratio of the ESC capacity to the capacity of the charging capacitor C_{ESC}/C_{CL} in the 100–120 range. This is a unique new feature of the developed device.

MATERIALS AND METHODS

Macroalgae *Ulva* sp. biomass

Green macroalgae *Ulva* sp. were collected, from Tel Aviv (Reading) areas during spring 2016. We chose to work with these species as they are known for the fast growth rates[62] and, thus, could provide us with rapid feedback on the system operation. In addition, these species are a potential feedstock for the biorefinery. Biomass was transported in the seawater filled plastic bags to the lab and sorted manually to get clean monocultures. Monocultures were cultivated/maintained in separate reactors as described in ref.[63] Nutrients were supplied by adding ammonium nitrate (NH_4NO_3, Haifa Chemicals Ltd, IS) and phosphoric acid (H_3PO_4, Haifa Chemicals Ltd, IS) to maintain 6.4 g m^{-3} of nitrogen and 0.97 g m^{-3} of phosphorus in the seawater.

Ulva sp. biomass Ohmic resistance determination

Ulva sp. biomass was harvested and centrifuged in the manual kitchen centrifuge to remove the surface water three times for 2 minutes. The biomass was loaded in the EPC, pressurized with the sliding electrodes, and exposed to the external electric field. The voltage drop was measured at the EPC and the resistor connected in series with a known resistance (5 Ohm). Voltages and currents were measured with a PicoScope 4224 Oscilloscope with a Pico Current Clamp (60 A AC/DC) and analyzed with Pico Scope 6 software (Pico technologies Inc., UK).

APPLICATION OF HIGH-VOLTAGE PEFS ON *ULVA* SP BIOMASS

Ulva sp. biomass (10 g) was loaded into the EPC. The 2 kg pressure was applied on the top sliding electrode using a metal block. Pulses were applied in the manual and computer-controlled modes. Currents and voltages on the cell were registered in real time with a PicoScope 4224 Oscilloscope with a Pico Current Clamp (60 A AC/DC) and analyzed with Pico Scope 6 software (Pico technologies Inc., UK). Extracted juice was collected at the bottom of the device. The experiment was repeated three times with fresh biomass.

ACKNOWLEDGMENTS

The authors thank the Israel Ministry of Science, Technology, and Space for the support of this work.

CONFLICT OF INTEREST

KL and AG have a patent application on the pulse generator topology.

REFERENCES

1. Palmeros Parada, M., Osseweijer, P. & Posada Duque, J.A. Sustainable biorefineries, an analysis of practices for incorporating sustainability in biorefinery design. *Ind. Crops Prod.* **106**, 105–123 (2017).
2. Bugge, M.M., Hansen, T. & Klitkou, A. What is the bioeconomy? A review of the literature. *Sustainability (Switzerland)* **8**, 691 (2016).
3. Meyer, R. Bioeconomy strategies: Contexts, visions, guiding implementation principles and resulting debates. *Sustain.* **9**, (2017).
4. Scarlat, N., Dallemand, J.F., Monforti-Ferrario, F. & Nita, V. The role of biomass and bioenergy in a future bioeconomy: Policies and facts. *Environ. Dev.* **15**, 3–34 (2015).
5. Espinoza Pérez, A.T., Camargo, M., Narváez Rincón, P.C. & Alfaro Marchant, M. Key challenges and requirements for sustainable and industrialized biorefinery supply chain design and management: A bibliographic analysis. *Renew. Sust. Energ. Rev.* **69**, 350–359 (2017).
6. Maity, S.K. Opportunities, recent trends and challenges of integrated biorefinery: Part II. *Renew. Sust. Energ. Rev.* **43**, 1446–1466 (2015).
7. Günerken, E. *et al.* Cell disruption for microalgae biorefineries. *Biotechnol. Adv.* **33**, 243–260 (2015).
8. Lee, S.Y., Cho, J.M., Chang, Y.K. & Oh, Y.K. Cell disruption and lipid extraction for microalgal biorefineries: A review. *Bioresour. Technol.* **244**, 1317–1328 (2017).
9. Mussatto, S.I. *Biomass Fractionation Technologies for a Lignocellulosic Feedstock Based Biorefinery*. *Biomass Fractionation Technologies for a Lignocellulosic Feedstock Based Biorefinery* (2016). doi:10.1016/C2014-0-01890-4
10. Rinaldi, R. Plant biomass fractionation meets catalysis. *Angew. Chemie—Int. Ed.* **53**, 8559–8560 (2014).
11. Golberg, A. *et al.* Energy efficient biomass processing with pulsed electric fields for bioeconomy and sustainable development. *Biotechnol. Biofuels* **9**, 1 (2016).
12. Flaumenbaum, B. Electrical treatment of fruits and vegetables before extraction of juice No Title. *Tr. OTIKP (in Russ).* **3**, 15–20 (1949).
13. Zagorulko, A. Technological parameters of beet desugaring process by the selective electroplosmolysis. *New Phys. Methods Foods Process. Moscow Izd. GosINTI,* 21–27 (1958).
14. Sack, M., Schultheiss, C. & Bluhm, H. Triggered Marx generators for the industrial-scale electroporation of sugar beets. *IEEE Trans. Ind. Appl.* **41**, 707–714 (2005).
15. Sack, M. *et al.* Research on industrial-scale electroporation devices fostering the extraction of substances from biological tissue. *Food Eng. Rev.* **2**, 147–156 (2010).
16. Lebovka, N.I., Shynkaryk, N.V. & Vorobiev, E. Pulsed electric field enhanced drying of potato tissue. *J. Food Eng.* **78**, 606–613 (2007).
17. Hossain, M.B., Aguiló-Aguayo, I., Lyng, J.G., Brunton, N.P. & Rai, D.K. Effect of pulsed electric field and pulsed light pre-treatment on the extraction of steroidal alkaloids from potato peels. *Innov. Food Sci. Emerg. Technol.* **29**, 9–14 (2015).
18. Boussetta, N., Grimi, N., Lebovka, N.I. & Vorobiev, E. 'Cold' electroporation in potato tissue induced by pulsed electric field. *J. Food Eng.* **115**, 232–236 (2013).
19. Luengo, E., Álvarez, I. & Raso, J. Improving carotenoid extraction from tomato waste by pulsed electric fields. *Front. Nutr.* **1**, 12 (2014).
20. Loginova, K.V., Lebovka, N.I. & Vorobiev, E. Pulsed electric field assisted aqueous extraction of colorants from red beet. *J. Food Eng.* **106**, 127–133 (2011).
21. Ma, S. & Wang, Z.H. Pulsed electric field-assisted modification of pectin from sugar beet pulp. *Carbohydr. Polym.* **92**, 1700–1704 (2013).
22. Jemai, A.B. & Vorobiev, E. Pulsed electric field assisted pressing of sugar beet slices: Towards a novel process of cold juice extraction. *Biosyst. Eng.* **93**, 57–68 (2006).
23. Cholet, C. *et al.* Structural and biochemical changes induced by pulsed electric field treatments on cabernet sauvignon grape berry skins: Impact on cell wall total tannins and polysaccharides. *J. Agric. Food Chem.* **62**, 2925–2934 (2014).
24. Medina-Meza, I.G. & Barbosa-Cánovas, G.V. Assisted extraction of bioactive compounds from plum and grape peels by ultrasonics and pulsed electric fields. *J. Food Eng.* **166**, 268–275 (2015).
25. Kotnik, T. *et al.* Electroporation-based applications in biotechnology. *Trends Biotechnol.* **33**, 480–488 (2015).
26. Yarmush, M.L., Golberg, A., Serša, G., Kotnik, T. & Miklavčič, D. Electroporation-based technologies for medicine: Principles, applications, and challenges. *Annu. Rev. Biomed. Eng.* **16**, 295–320 (2014).
27. Weaver, J.C. & Chizmadzhev, Y.A. Theory of electroporation: A review. *Bioelectrochem. Bioenerg.* **41**, 135–160 (1996).
28. Sack, M., Hochberg, M. & Mueller, G. Synchronized switching and active clamping of IGBT switches in a simple Marx generator. In *PCIM Europe 2016; International Exhibition and Conference for Power Electronics, Intelligent Motion, Renewable Energy and Energy Management* (2016).
29. Sack, M., Ruf, J., Hochberg, M., Herzog, D. & Mueller, G. A device for combined thermal and pulsed electric field treatment of food. In *2017 International Conference on Optimization of Electrical and Electronic Equipment (OPTIM) & 2017 Intl Aegean Conference on Electrical Machines and Power Electronics (ACEMP),* 31–36 (IEEE, 2017). doi:10.1109/OPTIM.2017.7974943
30. Reberšek, M., Miklavčič, D., Bertacchini, C. & Sack, M. Cell membrane electroporation-part 3: The equipment. *IEEE Electr. Insul. Mag.* **30**, 8–18 (2014).
31. Sungwoo Bae, Kwasinski, A., Flynn, M.M. & Hebner, R.E. High-power pulse generator with flexible output pattern. *IEEE Trans. Power Electron.* **25**, 1675–1684 (2010).
32. Lucia, O., Sarnago, H., Garcia-Sanchez, T., Mir, L.M. & Burdio, J.M. Industrial electronics for biomedicine: A new cancer treatment using electroporation. *IEEE Ind. Electron. Mag.* (2019). doi:10.1109/MIE.2019.2942377
33. Reberšek, M. & Miklavčič, D. Advantages and disadvantages of different concepts of electroporation pulse generation | Prednosti i nedostaci razlïcitih pristupa generiranja impulsa za elektroporaciju. *Automatika* (2011).
34. Chapter 16. Concepts of Electroporation Pulse Generation and Overview of Electric Pulse Generators for Cell and Tissue Electroporation | Semantic Scholar. https://www.semanticscholar.org/paper/Chapter-16.-Concepts-of-Electroporation-Pulse-and-Rebersek-Miklavčič/6127b0c7038e7e314fb2d7c70664ba6ce570e331
35. Jaroszeski, M.J., Heller, R., Gilbert, R. & Hofmann, G.A. Instrumentation and electrodes for in vivo electroporation. In *Electrochemotherapy, Electrogenetherapy, and Transdermal Drug Delivery* (2003). doi:10.1385/1-59259-080-2:37
36. Puc, M. *et al.* Techniques of signal generation required for electropermeabilization. Survey of electropermeabilization devices. *Bioelectrochemistry* 113–124 (2004). doi:10.1016/j.bioelechem.2004.04.001
37. Tseng, S.Y., Wu, T.F., Yang, H.R., Guo, J.C. & Hung, J.C. Soft-switching series-resonant converter to generate high output voltage for processing microbes. In *Conference Proceedings—IEEE Applied Power Electronics Conference and Exposition—APEC* (2004). doi:10.1109/apec.2004.1295930
38. Levkov, K., Vitkin, E., González, C.A. & Golberg, A. A laboratory IGBT-based high-voltage pulsed electric field generator for effective water diffusivity enhancement in chicken meat. *Food Bioprocess Technol.* (2019). doi:10.1007/s11947-019-02360-5

39. Ogugbue, C.J. & Sawidis, T. Bioremediation and detoxification of synthetic wastewater containing triarylmethane dyes by *Aeromonas hydrophila* isolated from industrial effluent. *Biotechnol. Res. Int.* (2011). doi:10.4061/2011/967925
40. Elgenedy, M.A., Darwish, A., Ahmed, S. & Williams, B.W. A transition arm modular multilevel universal pulse-waveform generator for electroporation applications. *IEEE Trans. Power Electron.* (2017). doi:10.1109/TPEL.2017.2653243
41. Elgenedy, M.A., Darwish, A., Ahmed, S. & Williams, B.W. A modular multilevel generic pulse-waveform generator for pulsed electric field applications. *IEEE Trans. Plasma Sci.* (2017). doi:10.1109/TPS.2017.2727068
42. Petkovsek, M. *et al.* High voltage pulse generation. *Electron. Lett.* **38**, 680–682 (2002).
43. Reberek, M. *et al.* Blumlein configuration for high-repetition-rate pulse generation of variable duration and polarity using synchronized switch control. *IEEE Trans. Biomed. Eng.* (2009). doi:10.1109/TBME.2009.2027422
44. Kohler, S., Couderc, V., O'Connor, R., Arnaud-Cormos, D. & Leveque, P. A versatile high voltage nano-and sub-nanosecond pulse generator. *IEEE Trans. Dielectr. Electr. Insul.* (2013). doi:10.1109/TDEI.2013.6571435
45. Tang, T., Wang, F., Kuthi, A. & Gundersen, M.A. Diode opening switch based nanosecond high voltage pulse generators for biological and medical applications. In *IEEE Transactions on Dielectrics and Electrical Insulation* (2007). doi:10.1109/TDEI.2007.4286519
46. Sarnago, H. *et al.* A versatile multilevel converter platform for cancer treatment using irreversible electroporation. *IEEE J. Emerg. Sel. Top. Power Electron.* (2016). doi:10.1109/JESTPE.2015.2512324
47. Bertacchini, C. *et al.* Design of an irreversible electroporation system for clinical use. *Technol. Cancer Res. Treat.* (2007). doi:10.1177/153303460700600408
48. Novickij, V. *et al.* High-frequency submicrosecond electroporator. *Biotechnol. Biotechnol. Equip.* (2016). doi:10.1080/13102818.2016.1150792
49. Flisar, K., Meglic, S.H., Morelj, J., Golob, J. & Miklavcic, D. Testing a prototype pulse generator for a continuous flow system and its use for *E. coli* inactivation and microalgae lipid extraction. *Bioelectrochemistry* (2014). doi:10.1016/j.bioelechem.2014.03.008
50. Grainys, A., Novickij, V. & Novickij, J. High-power bipolar multilevel pulsed electroporator. *Instrum. Sci. Technol.* (2016). doi:10.1080/10739149.2015.1060607
51. Garcia-Sanchez, T. *et al.* Successful tumor electrochemotherapy using sine waves. *IEEE Trans. Biomed. Eng.* (2019). doi:10.1109/tbme.2019.2928645
52. Buschmann, A.H. *et al.* Seaweed production: Overview of the global state of exploitation, farming and emerging research activity. *Eur. J. Phycol.* **52**, 391–406 (2017).
53. Fernand, F. *et al.* Offshore macroalgae biomass for bioenergy production: Environmental aspects, technological achievements and challenges. *Renew. Sustain. Energy Rev.* **75**, 35–45 (2016).
54. Jiang, R., Ingle, K.N. & Golberg, A. Macroalgae (seaweed) for liquid transportation biofuel production: What is next? *Algal Res.* **14**, 48–57 (2016).
55. Jung, K.A.A., Lim, S.-R.R., Kim, Y. & Park, J.M.M. Potentials of macroalgae as feedstocks for biorefinery. *Bioresour. Technol.* **135**, 182–190 (2013).
56. Robin, A., Chavel, P., Chemodanov, A., Israel, A. & Golberg, A. Diversity of monosaccharides in marine macroalgae from the Eastern Mediterranean Sea. *Algal Res.* **28**, 118–127 (2017).
57. Polikovsky, M. *et al.* Towards marine biorefineries: Selective proteins extractions from marine macroalgae *Ulva* with pulsed electric fields. *Innov. Food Sci. Emerg. Technol.* **37**, 194–200 (2016).
58. Postma, P.R. *et al.* Biorefinery of the macroalgae *Ulva lactuca*: Extraction of proteins and carbohydrates by mild disintegration. *J. Appl. Phycol.* 1–13 (2017). doi:10.1007/s10811-017-1319-8
59. Prabhu, M.S., Levkov, K., Livney, Y.D., Israel, A. & Golberg, A. High-voltage pulsed electric fields preprocessing enhances extraction of starch, proteins and ash from marine macroalgae *Ulva ohnoi*. *ACS Sustain. Chem. Eng.* (2019). doi:10.1021/acssuschemeng.9b04669
60. Prabhu, M. *et al.* Energy efficient dewatering of far offshore grown green macroalgae *Ulva* sp. biomass with pulsed electric fields and mechanical press. *Bioresour. Technol.* (2020). doi:10.1016/j.biortech.2019.122229
61. Robin, A. & Golberg, A. Pulsed electric fields and electroporation technologies in marine macroalgae biorefineries, 1–16 (2016). doi:10.1007/978-3-319-26779-1_218-1
62. Bruhn, A. *et al.* Bioenergy potential of *Ulva lactuca*: Biomass yield, methane production and combustion. *Bioresour. Technol.* **102**, 2595–604 (2011).
63. Chemodanov, A., Robin, A. & Golberg, A. Design of marine macroalgae photobioreactor integrated into building to support seagriculture for biorefinery and bioeconomy. *Bioresour. Technol.* **241**, 1084–1093 (2017).